IAI Journals.ASM.org

Surface Structure Characterization of *Aspergillus fumigatus* Conidia Mutated in the Melanin Synthesis Pathway and Their Human Cellular Immune Response

Jagadeesh Bayry,[a,b] Audrey Beaussart,[c] Yves F. Dufrêne,[c] Meenu Sharma,[a,b] Kushagra Bansal,[a,b] Olaf Kniemeyer,[d,e] Vishukumar Aimanianda,[f] Axel A. Brakhage,[d] Srini V. Kaveri,[a,b] Kyung J. Kwon-Chung,[g] Jean-Paul Latgé,[f] Anne Beauvais[f]

Institut National de la Santé et de la Recherche Médicale, Unité 1138, Paris, France[a]; Centre de Recherche des Cordeliers, Université Pierre et Marie Curie–Paris 6, Université Paris Descartes, Paris, France[b]; Université Catholique de Louvain, Institute of Life Sciences, Louvain-la-Neuve, Belgium[c]; Molecular and Applied Microbiology, Leibniz-Institute for Natural Product Research and Infection Biology, University of Jena, Jena, Germany[d]; Integrated Research and Treatment Center, Center for Sepsis Control and Care Jena, University Hospital, Jena, Germany[e]; Unité des Aspergillus, Institut Pasteur, Paris, France[f]; Molecular Microbiology Section, Laboratory of Clinical Infectious Diseases, National Institute of Allergy and Infectious Disease, National Institutes of Health, Bethesda, Maryland, USA[g]

In *Aspergillus fumigatus*, the conidial surface contains dihydroxynaphthalene (DHN)-melanin. Six-clustered gene products have been identified that mediate sequential catalysis of DHN-melanin biosynthesis. Melanin thus produced is known to be a virulence factor, protecting the fungus from the host defense mechanisms. In the present study, individual deletion of the genes involved in the initial three steps of melanin biosynthesis resulted in an altered conidial surface with masked surface rodlet layer, leaky cell wall allowing the deposition of proteins on the cell surface and exposing the otherwise-masked cell wall polysaccharides at the surface. Melanin as such was immunologically inert; however, deletion mutant conidia with modified surfaces could activate human dendritic cells and the subsequent cytokine production in contrast to the wild-type conidia. Cell surface defects were rectified in the conidia mutated in downstream melanin biosynthetic pathway, and maximum immune inertness was observed upon synthesis of vermelone onward. These observations suggest that although melanin as such is an immunologically inert material, it confers virulence by facilitating proper formation of the *A. fumigatus* conidial surface.

Melanin is a pigment that exists from humans to plants and has several functions, including resistance against environmental stress, such as UV light and oxidizing agents (1, 2). In airborne fungal spores, melanin helps in invasion of the host (3, 4) and contributes to the virulence of fungal pathogens (5, 6). Fungi produce different types of melanin: dihydroxynaphthalene (DHN)-melanin, pyomelanin, and DOPA-melanin. *Aspergillus fumigatus* produces the pigment DHN-melanin, responsible for the characteristic gray-green color of conidia. *A. fumigatus* is also able to produce a brownish pigment, pyomelanin, as an alternative melanin (7). Pyomelanin is produced via degradation of L-tyrosine with homogentisic acid as the main intermediate. On the other hand, *Cryptococcus neoformans* and *Paracoccidioides brasiliensis* synthesize DOPA-melanin (8). The production of melanin has been associated with the survival of the fungal species in the host (8, 9). DHN-melanin is hydrophobic and negatively charged, which modulates the binding capacity of conidia to host fibronectin and laminin present in the lungs (10). DHN-melanin is also essential for the proper assembly of cell wall layers in *A. fumigatus*. Pyomelanin was shown to protect the fungus from host defense mechanism, i.e., reactive oxygen intermediates and hence considered to be protecting the fungus against immune effector cells during infection (11). DOPA-melanin contributes to host death, fungal burden, and dissemination (8).

Genes responsible for the synthesis of DHN-melanin in *A. fumigatus* belong to a 19-kb cluster located on chromosome 2. Six genes have been identified in this cluster, and their functions were elucidated (Fig. 1) (4–6, 12–14). *PKSP* (*ALB1*; AFUA_2G17600) is the first gene of the pathway and codes for a polyketide synthase, which is responsible for catalyzing the synthesis of the heptaketide naphthopyrone from acetyl coenzyme A (acetyl-CoA) and malonyl-CoA. The heptaketide is then shortened by hydrolysis, reduction and dehydration by Ayg1p (AFUA_2G17550), Arp2p (AFUA_2G17560), and Arp1p (AFUA_2G17580), respectively. The generated product 1,3,6,8-tetrahydroxynaphthalene is reduced again by Arp2p and the resulting vermelone is oxidized by the copper oxidase Abr1p (AFUA_2G17540) to form the 1,8-DHN-melanin, which is polymerized by the laccase Abr2p (AFUA_2G17530) (12, 15).

The role of the conidial melanin in the *A. fumigatus* virulence has been studied by using either melanin ghosts or the pigmentless mutant, wherein the *PKSP* gene, which encodes a protein involved in the first step of melanin biosynthesis, has been deleted (4, 9, 16–19), These reports demonstrated that melanin protects the conidia against reactive oxygen species, masks the recognition of various *A. fumigatus* pattern-associated molecular patterns, inhibits macrophage apoptosis and phagolysosome fusion, and attenuates the host immune response. All of these functions of melanin contribute to the increased survival of conidia in macrophages and promote the dissemination of *A. fumigatus* within the host.

However, the importance of melanin in the organization of the *A. fumigatus* conidial cell wall, the structural organization of the

Received 6 March 2014 Returned for modification 17 March 2014
Accepted 5 May 2014
Published ahead of print 12 May 2014
Editor: G. S. Deepe, Jr.
Address correspondence to Jean-Paul Latgé, jean-paul.latge@pasteur.fr, or Anne Beauvais, anne.beauvais@pasteur.fr.

doi:10.1128/IAI.01726-14

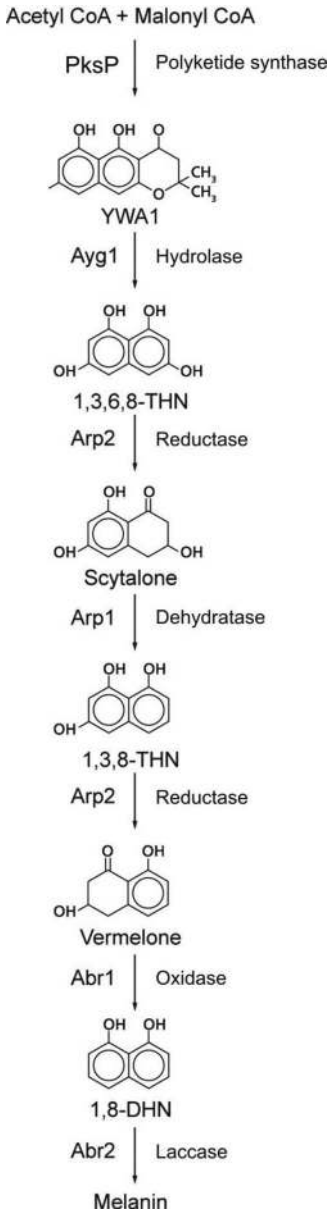

FIG 1 Schematic representation of melanin biosynthetic pathway.

conidial surface due to the lack of melanin or in the presence of melanin intermediates, and the effect of melanin intermediate biosynthetic gene deletion on the activation of host immune cells are still unknown. In the present study, by using melanin mutants that are deleted in each of the genes of the melanin synthesis pathway, we analyzed the surface structure of conidia by biochemical and biophysical methods and explored the immunomodulatory role of these conidia on human dendritic cells (DCs), the professional antigen-presenting cells that act as sentinels of the immune system. We demonstrate for the first time that until the scytalone precursor was synthesized by Arp2p, the first three melanin biosynthetic gene deletion mutants (Δ*pksP*, Δ*ayg1*, and Δ*arp2*) induce the maturation of DCs and cytokine production. Upon vermelone biosynthesis after dehydratation of the scytalone by Arp1p and reduction by Arp2, the subsequent mutants (Δ*abr1* and Δ*abr2*) behaved like wild-type (WT) conidia, losing their capacity to prime the maturation of DCs and cytokine production. The Δ*arp1* conidia having scytalone but not vermelone on their surfaces were able to induce only a weak maturation of DCs. Further, we found that activation of DCs by Δ*pksP*, Δ*ayg1*, and Δ*arp2* conidia was in part due to amorphous proteinaceous conidial surface with patchy rodlets or surface exposed other cell wall components. Δ*arp1* conidia phenotype was intermediate between Δ*arp2* and Δ*abr1*, whereas Δ*abr1*, Δ*abr2*, and WT conidia lack such material and have conidial surfaces covered with rodlets, which contribute for the masking of conidial recognition by the innate immune cells.

MATERIALS AND METHODS

Fungal strains and culture conditions. The melanin precursor Δ*pksP*, Δ*ayg1*, Δ*arp2*, Δ*arp1*, Δ*abr1*, and Δ*abr2* mutant strains and the WT strain B5233 have been maintained in silica gel at J. Kwon-Chung's laboratory at the National Institutes of Health until use (6, 14, 15). All strains were cultivated on malt-agar (2%) medium at ambient temperature for at least 15 days before collecting the resting conidia. Conidia were harvested from the culture medium using 0.05% Tween 20 in water. Conidial suspensions were filtered using BD Falcon filters (BD Biosciences) to remove any mycelium. For immunolabeling and DC experiments, resting conidia were fixed with paraformaldehyde (PFA)-fixed (2.5% [vol/vol] PFA in phosphate-buffered saline [PBS]) overnight at 4°C. The fixed conidia were subsequently washed three times with 0.1 M NH_4Cl and once with PBS–0.1% Tween 20.

Melanin extraction. The isolation of melanin from the WT conidia was performed as previously described (20, 21). After the fungi were gown on malt-agar medium for 15 days at ambient temperature, the conidia of each strain were collected in 0.05% Tween-water. Briefly, conidia were treated with a combination of proteolytic (proteinase K; Sigma) and glycohydrolytic (Glucanex; Novo) enzymes, denaturant (guanidine thiocyanate), and hot, concentrated HCl (6 M). This treatment resulted in an electron-dense layer similar in size and shape to the original conidial melanin layer without underlying cell components, for which reason these electron-dense materials were called "melanin ghosts" (20).

Extraction of the AS polysaccharide fraction from conidia. Conidia were disrupted with 0.5-mm-diameter glass beads in a FastPrep (MP Biomedicals). The conidial cell wall fraction was recovered by centrifugation, washed with water, and then freeze-dried. The dried cell wall fraction was boiled in 50 mM Tris-HCl (pH 7.4) containing 50 mM EDTA, 2% sodium dodecyl sulfate (SDS), and 40 mM β-mercaptoethanol (10 min, twice) to remove proteins and extensively washed with water to obtain cell wall polysaccharides. From the latter, the alkali-soluble (AS) fraction was extracted as described earlier (22).

Extraction of conidial surface RodA protein (RodAp) involved in rodlet formation. RodAp was extracted from the spore surface by incubating 10^9 dry conidia with 48% (vol/vol) hydrofluoric acid (HF) for 72 h at 4°C (23). The contents were centrifuged (10,000 × *g*, 10 min), and the supernatant obtained was dried under N_2. The dried material was reconstituted in H_2O, and an aliquot was subjected to SDS-PAGE (15% [wt/vol]) analysis and visualized by silver nitrate staining.

Analysis of proteins on the conidial surface. Conidia were incubated in 0.5 M NaCl solution for 2 h at room temperature at a ratio of 10^{10} conidia per ml. The NaCl supernatant was recovered after centrifugation and directly subjected to SDS-PAGE (10% [wt/vol]). Two-dimensional (2D) gel electrophoretic analysis of the NaCl extract was carried out as described previously with slight modifications (24, 25). A 50- to 100-μg portion of protein was loaded onto IPG strips (11 cm, pH 3 to 7; GE Healthcare Life Sciences) by in-gel rehydration. After equilibration of the IPG strips, SDS-gel electrophoresis was carried out using Criterion AnykD TGX Stain-Free precast gels (Bio-Rad). Proteins were visualized by UV light and colloidal Coomassie blue staining (Candiano2004). After

scanning, the gel images were analyzed with the software Delta 2D 4.3 (Decodon). Protein spots were excised and analyzed by mass spectrometry using an ultrafleXtreme MALDI-TOF/TOF device (Bruker Daltonics) as described previously (26).

Analysis of carbohydrate on the conidial surface by fluorescence microscopy. The mannose moieties of glycoproteins on the resting conidial surface were labeled with concanavalin-fluorescein isothiocyanate (ConA-FITC; Sigma) at 0.1 mg/ml after incubating the resting conidia for 1 h at 37°C in 0.1 M carbonate buffer (pH 9.6) containing 0.1% Tween 20. The hexosamines were labeled with wheat germ agglutinin (WGA)-FITC at 0.1 mg/ml upon incubating the resting conidia for 1 h at the room temperature in PBS containing 0.1% Tween 20. For immunolabeling, PFA-fixed conidia were incubated with different antibodies as described previously (27). β-(1,3)-Glucan was labeled with dectin-1 (Fc-dectin1, 6 μg/ml), followed by FITC-conjugated GaHu-Fab2-human IgG (5 μg/ml; kindly provided by G. Brown, University of Aberdeen, Aberdeen, United Kingdom) (28).

Antibodies and reagents for human immunology. Recombinant human granulocyte-macrophage colony-stimulating factor (GM-CSF) and interleukin-4 (IL-4) were from Miltenyi Biotec (France). Fluorescein isothiocyanate (FITC)-conjugated monoclonal antibodies (MAbs) to CD80 and phycoerythrin (PE)-conjugated MAbs to CD83 and CD86 were from BD Biosciences (France), and PE-conjugated MAb to CD40 was from Becton Dickinson (France). Anti-Thr202/Tyr204 phospho-extracellular signal-related kinase 1/2 (ERK1/2) and anti-Thr180/Tyr182 phospho-p38 mitogen-activated protein (MAPK) antibodies were purchased from Cell Signaling Technology (USA). Anti-β-actin antibody (AC-15) was from Sigma-Aldrich (USA).

Generation and culture of human DCs. Monocyte-derived DCs were generated as previously described (29, 30). Immature DCs (0.5×10^6 cells/well/ml) were cultured in the presence of GM-CSF and IL-4 (cytokines) alone, with cytokines and PFA-fixed conidia of the wild type or melanin mutants (1:1 ratio), with cytokines and 1 μg of melanin extracts, with cytokines and 1 μg of AS polysaccharide fraction of *A. fumigatus* cell wall (positive control), or with cytokines and NaCl extracts from 0.75×10^9 conidia for 48 h. Cells were harvested, and cell-free supernatants were stored at −80°C for cytokine analysis. Cells were labeled with fluorochrome-conjugated MAbs for surface marker analysis by using LSR II flow cytometry (BD Biosciences). Five thousand events were recorded for each sample, and data were analyzed by BD FACS DIVA software (BD Biosciences).

Mixed lymphocyte reaction. $CD4^+$ T cells were isolated from peripheral blood mononuclear cells of healthy donors using CD4 microbeads (Miltenyi Biotec). DCs were washed extensively and cocultured with 10^5 responder $CD4^+$ T cells at DC/T cell ratios of 1:10, 1:20, 1:40, and 1:80. After 4 days, either cells were harvested and cell-free supernatants were stored at −80°C for cytokine analysis, or cells were pulsed for 16 to 18 h with 0.5 μCi of [^{3}H]thymidine. Radioactive incorporation was measured by standard liquid scintillation counting. The proliferation of cells was measured as mean counts per minute (cpm) ± the standard error of the mean (SEM) of quadruplicate values after subtracting the values of responder T cell cultures alone.

Measurement of cytokines. Cytokines were quantified in cell-free culture supernatants using CBA human inflammation and human Th1/Th2 kits (BD Biosciences).

Statistical analysis. A two-sided, Student-*t* test was used for statistical analysis. A *P* value of <0.05 was considered significant (*, $P < 0.05$; **, $P < 0.01$).

Immunoblotting. Immunoblotting was performed as described previously (31). DCs were washed with ice-cold PBS in radioimmunoprecipitation assay lysis buffer (50 mM Tris-HCl [pH 7.4]; 1% NP-40; 0.25% sodium deoxycholate; 150 mM NaCl; 1 mM EDTA; 1 mM phenylmethylsulfonyl fluoride; 1 μg of aprotinin, leupeptin, and pepstatin/ml; 1 mM Na_3VO_4; 1 mM NaF). Equal amounts of proteins from the total cell lysates were subjected to SDS-PAGE, followed by transfer of proteins to polyvinylidene difluoride membranes. Membranes were blocked in TBST buffer (0.02 M Tris-HCl [pH 7.5], 0.15 M NaCl, 0.1% Tween 20) containing 5% nonfat dried milk and investigated using a primary antibody overnight at 4°C. After washing with TBST, membranes were incubated with horseradish peroxidase-conjugated secondary antibody (Jackson Immunologicals, USA). The blots were then developed with an enhanced chemiluminescence detection system (Perkin-Elmer, USA) according to the manufacturer's instructions.

Analysis of the conidial surface by AFM. Conidial surfaces were analyzed by atomic force microscopy (AFM) using a Multimode VIII instrument (Bruker, Santa Barbara, CA). Sample immobilization was achieved by mechanically trapping living conidia into porous polycarbonate membranes (it4ip SA; Belgium). After a concentrated suspension of cells was filtered, the membrane was rinsed with deionized water, carefully cut, and attached to a metallic puck using double-sided tape. The mounted sample was then transferred to the AFM liquid cell, while avoiding dewetting. Imaging was performed in contact mode under minimal applied force using oxide-sharpened microfabricated Si_3N_4 cantilevers (MSCT; Bruker) with a nominal spring constant of 0.01 N/m. Force measurements were carried out by chemical-force microscopy (32, 33) using gold tips (OMCL-TR4; Olympus, Tokyo, Japan) coated with hydrophobic thiols. To do so, cleaned tips were immersed for 12 h in 1 mM solutions of $HS(CH_2)_{11}CH_3$ (Sigma) in ethanol, rinsed, and dried with N_2 prior to use. The cantilevers spring constants were measured by the thermal noise method (Picoforce; Bruker). Force curves were analyzed in order to determine the adhesion force between the conidia and the AFM tip. These adhesion forces were plotted as bright pixels, with brighter colors indicating larger adhesion values. The data were processed using Nanoscope analysis (Bruker) and MATLAB software (MathWorks, Natick, MA). For each strain, several images were obtained on different conidia, and force measurements were obtained in duplicate using different tips.

RESULTS

***A. fumigatus* conidia from Δ*pksP*, Δ*ayg1*, and Δ*arp2* mutants induce maturation and activation of human DCs.** Conidia from individual melanin biosynthetic pathways gene deletion mutants were used to study the maturation and activation of DCs. Melanin-mutant conidia deficient in the early steps of the biosynthetic pathway (Δ*pksP*, Δ*ayg1*, and Δ*arp2*) induced the maturation of DCs, as demonstrated by the significantly enhanced expression of CD83 and costimulatory molecules CD86, CD80, and CD40 (Fig. 2) (34, 35). The Δ*pksP*, Δ*ayg1*, and Δ*arp2* conidia also stimulated a panel of DC-cytokines such as tumor necrosis factor alpha (TNF-α), IL-1β, IL-6, and IL-10 (Fig. 3). Upon vermelone biosynthesis, the subsequent downstream melanin biosynthetic pathway mutant conidia (Δ*abr1* and Δ*abr2*) behaved like the WT strain, becoming immunologically inert (Fig. 2 and 3). The Δ*arp1* conidia presented an intermediate phenotype, since they induced only modest changes in the expression of costimulatory molecules of DCs and the secretion of DC-cytokines (Fig. 2 and 3).

Melanin does not stimulate DC maturation. As shown in Fig. 4, melanin ghosts from WT conidia did not induce DC maturation (Fig. 4A). We further verified the lack of activation of DCs by analyzing the intracellular signaling pathways and the ability of DCs to induce T cell proliferation and cytokines (Fig. 4B to D). We show that melanin ghost failed to phosphorylate p38 MAPK and ERK, thus confirming the immunological inert nature of melanin (Fig. 4B). The lack of activation of DCs by WT ghost extract was also reflected in the inability of WT ghost extract-treated DCs to promote T cell proliferation (Fig. 4C) and the T cell cytokines IL-2, interferon gamma (IFN-γ), and IL-5 (Fig. 4D). In contrast, the AS polysaccharide fraction [rich in α-(1,3)-glucan] of the *A. fumigatus* cell wall, used as a positive control, induced maturation

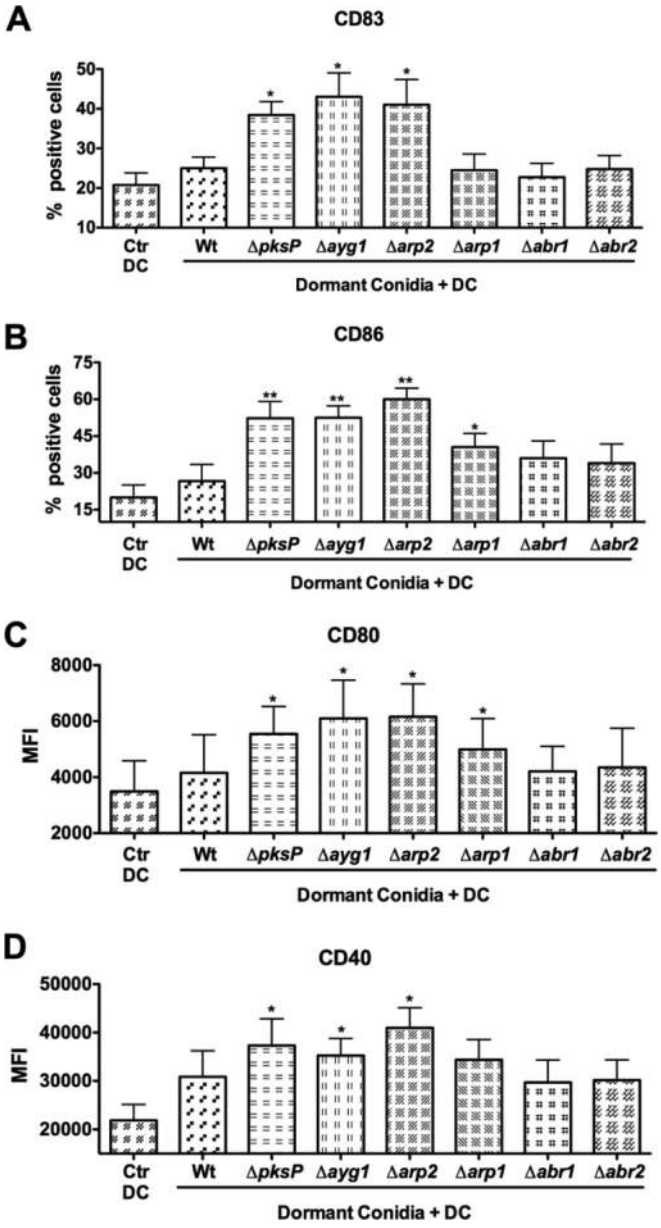

FIG 2 Effect of melanin biosynthetic pathways mutant conidia on the maturation of human DCs. Immature DCs (0.5×10^6 cells/ml) were cultured in the presence of cytokines GM-CSF and IL-4 (Ctr DC) or with cytokines and WT conidia or melanin biosynthetic pathway mutant conidia (Δ*pksP*, Δ*ayg1*, Δ*arp2*, Δ*arp1*, Δ*arb1*, and Δ*arb2*) at a 1:1 ratio for 48 h. The percent expression of CD83 (A) and CD86 (B) and the mean fluorescence intensities (MFI) of CD80 (C) and CD40 (D) were analyzed by flow cytometry. The data (means ± the SEM) are from four to five donors. The level of statistical significance is indicated (*, $P < 0.05$; **, $P < 0.01$).

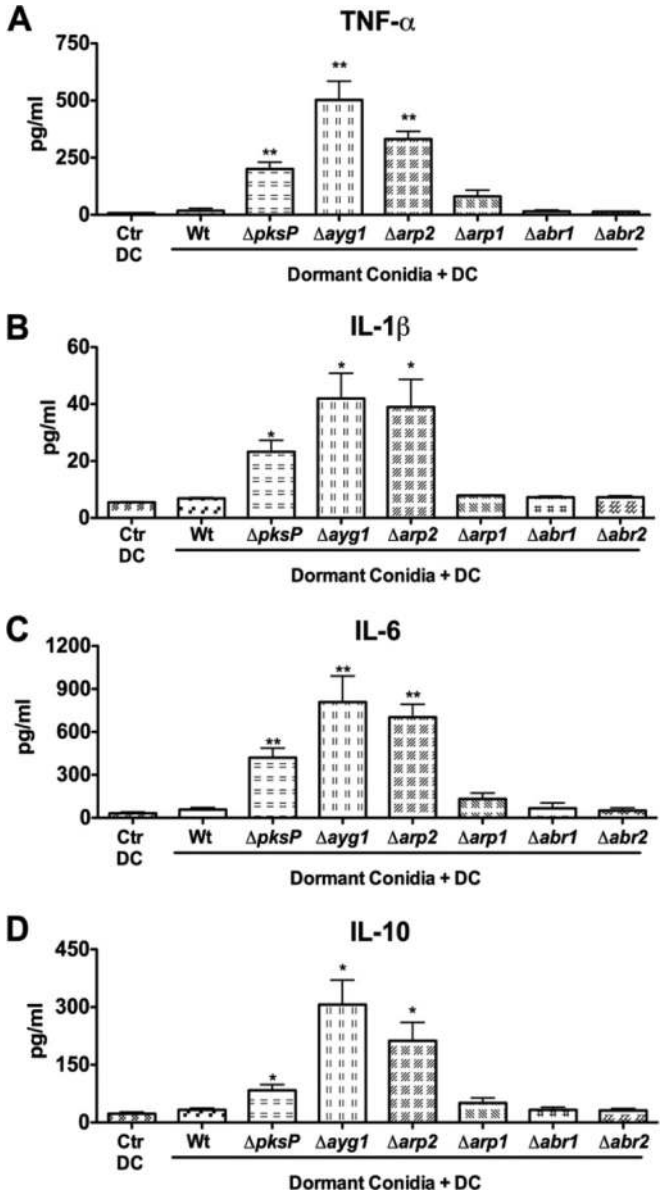

FIG 3 Induction of DC cytokines by the melanin biosynthetic pathways mutant conidia. Immature DCs (0.5×10^6 cells/ml) were cultured in the presence of cytokines GM-CSF and IL-4 (Ctr DC) or with cytokines and WT conidia or melanin biosynthetic pathway mutant conidia (Δ*pksP*, Δ*ayg1*, Δ*arp2*, Δ*arp1*, Δ*arb1*, and Δ*arb2*) at a 1:1 ratio for 48 h. Cell-free culture supernatants were analyzed for the secretion of TNF-α (A), IL-1β (B), IL-6 (C), and IL-10 (D). The data (means ± the SEM) are from four donors and are presented as pg/ml. The level of statistical significance is indicated (*, $P < 0.05$; **, $P < 0.01$).

of DCs, activated intracellular signaling pathways, and promoted DC-mediated T cell proliferation and cytokine production (Fig. 4). Taken together, these data indicated that conidial surface melanin, either *in situ* or in the extracted form (melanin ghosts), failed to stimulate DC activation and cytokine production.

The surface rodlet layer is masked by an amorphous hydrophilic layer. To investigate whether the structural modifications in the Δ*pksP*, Δ*ayg1*, Δ*arp2*, and Δ*arp1* conidia could be responsible for stimulating the DCs, conidial surfaces were imaged by AFM (36, 37) (Fig. 5A to O). Rather than using an incident beam as in classical microscopy, AFM probes the small forces acting on the sample surface (37). Three-dimensional images are generated in buffer by scanning a sharp tip over the cell surface while sensing the interaction force between the tip and the surface. Originally invented for topographic imaging, AFM has evolved into a multifunctional molecular toolkit, enabling researchers not only to observe structural details of cells to near molecular resolution (36, 38) but also to measure their biophysical properties and interac-

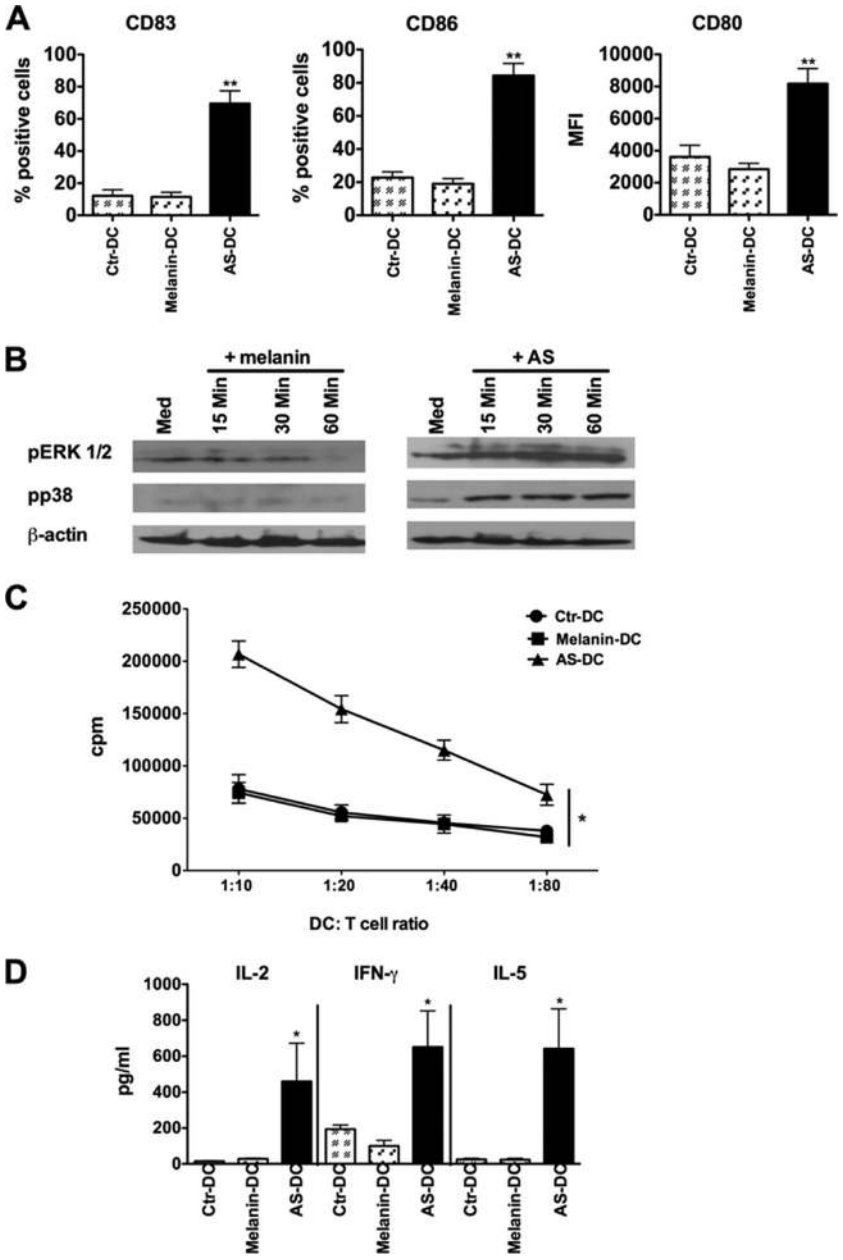

FIG 4 Effect of dihydroxynaphthalene (DHN)-melanin on the phenotype, intracellular signaling pathways, and T cell stimulatory abilities of DCs. (A) Immature DCs (0.5×10^6 cells/ml) were cultured in the presence of cytokines GM-CSF and IL-4 (negative control, Ctr-DC) or with cytokines and 1 μg of DHN-melanin from WT conidia (Melanin-DC) or 1 μg of the AS polysaccharide fraction of *A. fumigatus* cell wall (AS-DC, positive control) for 48 h. The percent expression of CD83 and CD86 and the mean fluorescence intensity (MFI) of CD80 were analyzed by flow cytometry. The data (means ± the SEM) are from four donors. (B) DCs were treated with 1 μg of DHN-melanin from WT conidia (left panels) or 1 μg of the AS polysaccharide fraction of *A. fumigatus* cell wall (AS, positive control; right panels) for the indicated time periods. The phosphorylation of ERK1/2 (pERK1/2) and p38 MAPK (pp38) was analyzed by immunoblotting. Med, unstimulated conditio. (C) DCs were cultured in the presence of the cytokines GM-CSF and IL-4 (negative control, Ctr-DC) or cytokines and 1 μg of melanin extracts from WT conidia or cytokines and 1 μg of the alkali-soluble (AS) fraction (positive control, AS-DC) for 48 h. After extensive washing, DCs were cocultured with $CD4^+$ T cells at various DC/T cell ratios. The T cell proliferation was quantified by measuring [^{3}H]thymidine incorporation, and values are presented as cpm. (D) $CD4^+$ T cell cytokines IL-2, IFN-γ, and IL-5 in the DC-T cell cocultures described above were quantified and are presented as pg/ml. The data (means ± the SEM) are from four donors. The level of statistical significance is indicated (*, $P < 0.05$; **, $P < 0.01$).

tions (39–41). In contrast to the WT conidia that are covered with rodlet structure (30, 42) (Fig. 5M to O), the Δ*pksP* mutant conidial surface was amorphous, without organized rodlet structure (Fig. 5A to C). Some patches of organized rodlet layers were observed on the Δ*ayg1* conidial surface (Fig. 5D to F), and their percentage increased on Δ*arp2* conidia (Fig. 5G to I) to finally cover almost the entire surface of the Δ*arp1* conidia (Fig. 5J to L). However, the rodlet layer on Δ*arp1* conidia appeared to be less compact and less organized than that of the WT conidia (Fig. 5M and O). The mutants of further downstream melanin biosynthetic

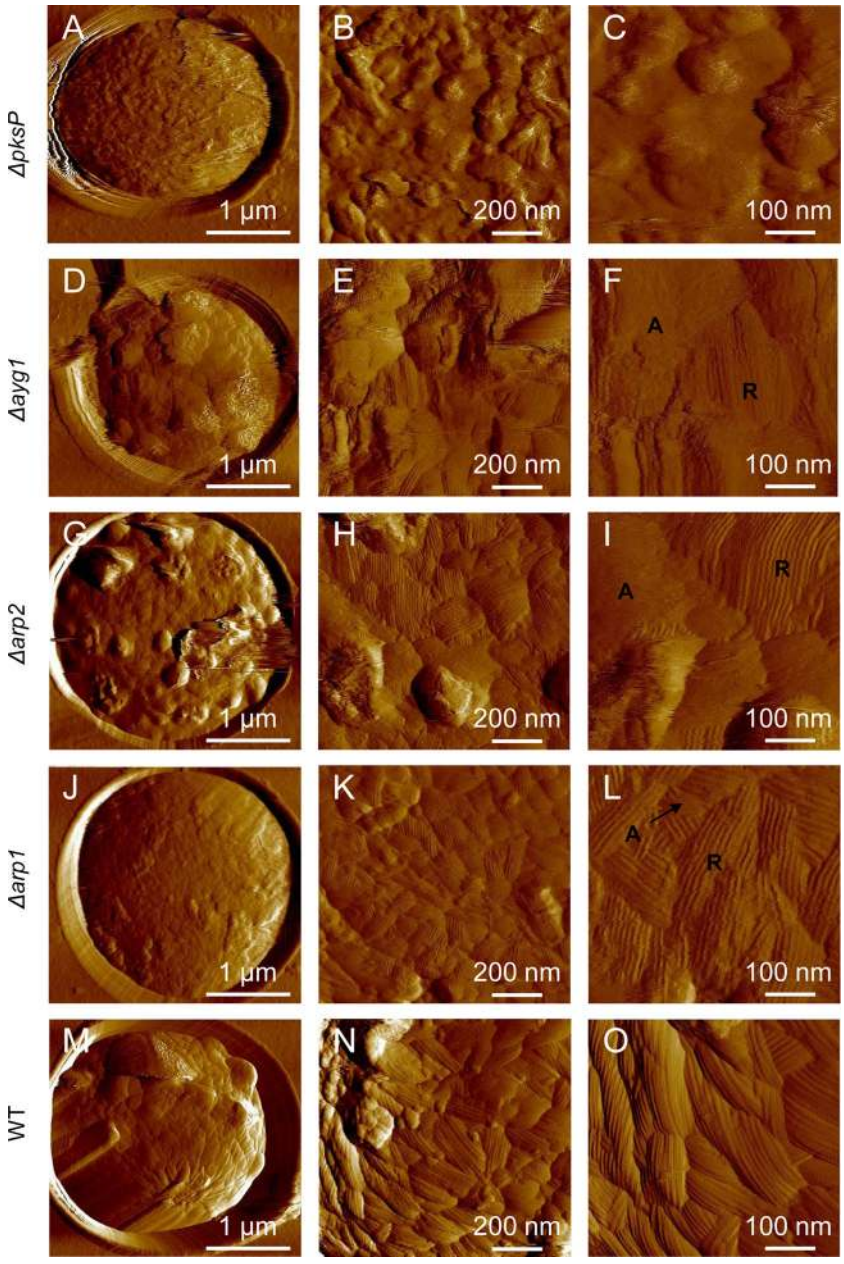

FIG 5 AFM imaging reveals that the loss of melanin correlates with the lack of exposed rodlet layer. AFM deflection images of the surfaces of Δ*pksP* (A to C), Δ*ayg1* (D to F), Δ*arp2* (G to I), Δ*arp1* (J to L), and WT (M to O) conidia recorded in deionized water at low (A, D, G, J, and M), medium (B, E, H, K, and N), and high (C, F, I, L, and O) resolutions. Black labels "R" and "A" indicate regions made of rodlets and amorphous materials, respectively.

pathway genes (Δ*abr1* and Δ*abr2*) presented organized and compact rodlets on the entire surface of their conidia, similar to WT conidia (data not shown).

To investigate whether RodAp (responsible for the formation of rodlet layer on the conidial surface) is still present on the Δ*pksP* mutant conidial surface, all of the mutant conidia, as well as the WT conidia, were treated with HF (30). RodAp could be extracted from the Δ*pksP* mutant, other melanin mutants, and WT conidia. Their SDS-PAGE profiles (Fig. 6) showed that two bands of RodAp classically seen in the HF extracts of conidia were present in all of the melanin pathway mutants and WT conidia (30). A band at 18 kDa could also be observed in Δ*pksP*, Δ*ayg1*, and Δ*arp2* HF extracts (Fig. 6). Mass spectrometry (MS) and tandem MS (MS/MS) analyses showed that this 18-kDa protein corresponds to the Aspf1 antigen, suggesting the loose architecture of rodlets in these mutants. These data confirmed AFM observations that the RodAp were present but hidden by an amorphous material on the surfaces of Δ*pksP*, Δ*ayg1*, and Δ*arp2* mutant conidia.

Because the presence of this amorphous material covers the hydrophobic rodlets, we sought to determine whether the observed surface changes correlated with differences in the conidial hydrophobic adhesive properties. To understand this, we mapped and quantified the nanoscale adhesion properties of WT and Δ*pksP* mutant conidia by AFM with hydrophobic tips. The pres-

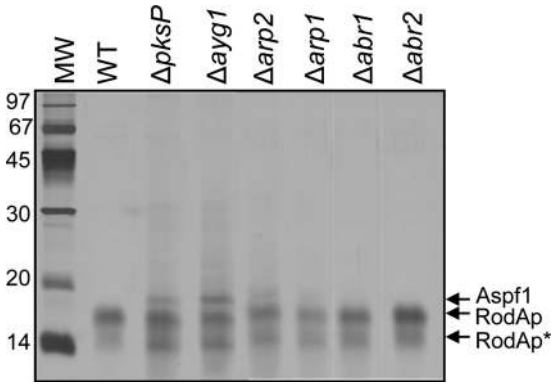

FIG 6 SDS-PAGE (15% gel) profile of the RodAp extracted from the WT and melanin biosynthetic pathway mutant conidial surfaces using hydrofluoric acid (HF). Protein bands were revealed by silver staining. RodAp*, degraded form of RodAp due to HF treatment.

ence of this unorganized material on the Δ*pksP* mutant conidial surface was associated with a dramatic reduction in their conidial surface hydrophobicity (Fig. 7). For the WT, force-distance curves recorded across the cell surface revealed large adhesion forces, ranging from 0.2 to 6 nN (Fig. 7M to O). In contrast, structural changes in Δ*pksP* conidia caused profound modifications in the cell surface physicochemical properties (Fig. 7A to C). Force-distance curves and force maps showed the absence of adhesion forces over the entire surface of the Δ*pksP* mutant conidia, indicating that this mutant is hydrophilic. The adhesion force of the other mutants of the melanin pathway increased with the rank of the mutant in the pathway, from a low adhesion with the Δ*pksP* and Δ*ayg1* conidia (Fig. 7A to F) to a maximal adhesion with WT conidia (Fig. 7M to O). The low adhesion capacities of the Δ*pksP*, Δ*ayg1*, and Δ*arp2* conidia indicated a modification of the cell surface hydrophobicity that could have influenced conidial recognition by DCs.

Proteins are present in the amorphous hydrophilic layer of Δ*pksP* and Δ*ayg1* mutant conidia. We then investigated the chemical nature of the amorphous layer present on the surfaces of Δ*pksP*, Δ*ayg1*, and Δ*arp2* mutant conidia. A strong labeling with ConA was observed only with the Δ*pksP* conidia, suggesting that its surface layer is rich in glycoconjugates. However, labeling with ConA was either low or negative in other melanin mutants, including Δ*ayg1* and Δ*arp2* mutants, and WT conidia (Fig. 8; data not shown). The surface amorphous material could be extracted by incubating mutant conidia (mutants for the initial steps of melanin biosynthesis) with 0.5 M NaCl for 2 h, and they were positive for protein test, suggesting the presence of glycoproteins in this conidial surface amorphous material. As shown in Fig. 9, the amount of proteins present in the extract was very high in Δ*pksP* mutant, followed by Δ*ayg1* mutant. Extract from Δ*pksP* mutant contained 53 μg of protein per 3×10^9 conidia, whereas Δ*ayg1* conidial extract contained 12 μg of protein. The surface extracts of other mutants conidia, i.e., Δ*arp2* and Δ*arp1* mutants contained 3.8 μg of protein, while in Δ*abr1*, Δ*abr2* and WT extracts the amount of proteins was too low to detect. These results thus indicate that smaller amounts of proteins on the surface layers of Δ*ayg1*, Δ*arp2*, and Δ*arp1* conidia reflected in the low or negative ConA-FITC staining of these conidia.

Extracted protein mixture of Δ*pksP* mutant was then subjected to proteomic analysis. Forty-one proteins were identified in the extract, and *in silico* analysis of these proteins by SigPred (http://www.cbs.dtu.dk/services/SignalP/) and CADRE (http://www.cadre-genomes.org.uk/Aspergillus_fumigatus/) revealed that all of them had a signal peptide (Table 1). Extracellular proteins, normally secreted during the vegetative growth of *A. fumigatus*, such as Cat1p, Exg1p, ExoG2p, Aspf1p, and ChiB1, were identified in the NaCl extract of Δ*pksP* resting conidia (43–46). Of the 41 proteins, nine were glycosylhydrolases. RodAp was also identified in the NaCl extract. Other proteins, such as proteasome components, translation elongation factors, pyruvate dehydrogenases, adenosine deaminase, and protein disulfide isomerase, normally found in intracellular compartments were present in very small amounts since they were identified only once or twice in the proteomic survey.

In order to determine whether the proteins present on the surface of Δ*pksP* and Δ*ayg1* conidia are responsible for the activation of DC by these mutant conidia, we incubated DCs with the NaCl extracts of Δ*pksP*, Δ*ayg1*, Δ*arp2*, and Δ*arp1* mutant and WT conidia. As expected, NaCl extract of Δ*pksP* and Δ*ayg1* mutants induced the maturation of DCs, whereas NaCl extracts of Δ*arp2*, Δ*arp1*, and WT strains did not (Fig. 10). These results demonstrated that the surface protein layer was responsible at least in part for the induction of DC maturation following incubation of cells with resting conidia of Δ*pksP* and Δ*ayg1* mutants. However, the amount of proteins present on the surfaces of Δ*arp2* and Δ*arp1* conidia was too low to stimulate DCs (Fig. 10). Although NaCl extracts from Δ*pksP* and Δ*ayg1* mutant conidial surfaces induced maturation of the DCs based on the phenotype analysis of cells (Fig. 10), they did not induce the production of cytokines such as IL-1β, IL-10, or IL-6 (data not shown). The level of production of above cytokines was on par with that of control DCs. These data suggest that signals provided by NaCl extracts of Δ*pksP* and Δ*ayg1* mutant conidia were not sufficient to induce the functional activation of the DCs. On the other hand, Δ*pksP*, Δ*ayg1*, and Δ*arp2* mutant conidia induced various DC cytokines, which could be due to the exposure of cell wall polysaccharides on their conidial surfaces.

Glucosamine-containing components are exposed at the Δ*pksP*, Δ*ayg1*, and Δ*arp2* conidial surfaces. To check whether any structural cell wall modification occurred and was responsible for DC activation by Δ*pksP*, Δ*ayg1*, and Δ*arp2* conidia, we labeled mutant and WT conidia with the β-(1,3)-glucan receptor dectin-1 and with the glucosamine (GlcN) recognizing lectin WGA. Mutants and WT conidia did not bind to dectin-1 (data not shown), suggesting that β-(1,3)-glucans were not exposed at the conidial surfaces. However, Δ*pksP*, Δ*ayg1*, and Δ*arp2* conidia were positive for WGA-FITC (Fig. 11), whereas Δ*abr1*, Δ*abr2*, and WT conidia were 3 to 9% WGA-FITC positive (Fig. 11). In line with the partial stimulation of DCs, Δ*arp1* mutant presented an intermediate phenotype: ca. 40% of the conidia were WGA positive. These results suggested that conidia with uniform exposure of glucosamine-containing components on the surface (in cases of Δ*pksP*, Δ*ayg1*, and Δ*arp2* mutant conidia) were able to induce DC activation, whereas conidia with low levels of exposure of GlcN content on the surface did not stimulate DCs (Δ*abr1*, Δ*abr2*, and WT). When GlcN exposure was intermediate as in Δ*arp1* conidia, such conidia were able to induce partial activation of DCs.

Consequently, the absence of melanin or at least of the intermediate scytalone increased the permeability of the conidia to

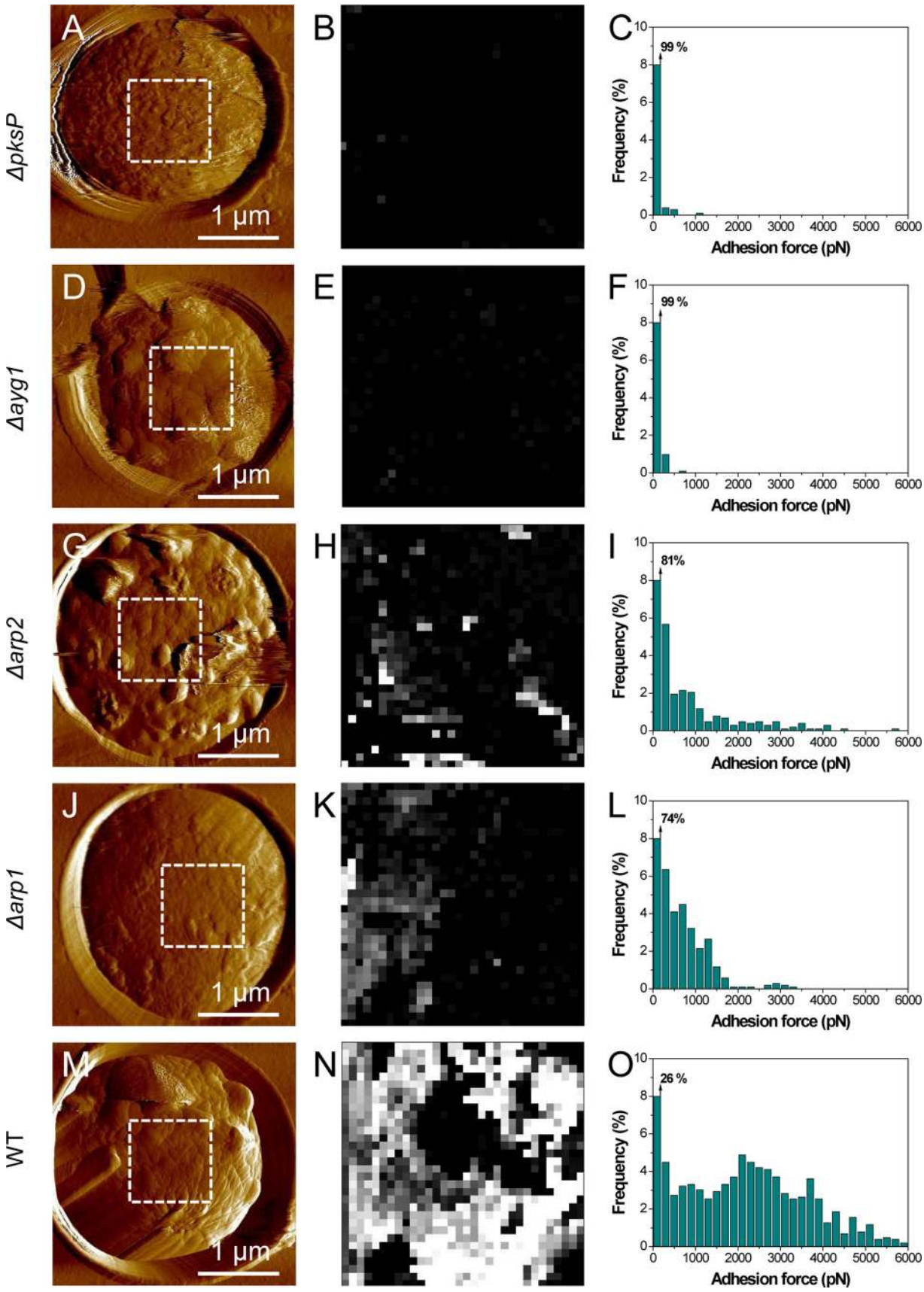

FIG 7 Structural modifications influence the conidial surface hydrophobicity. AFM deflection images (A, D, G, J, and M) recorded in deionized water, together with adhesion force maps (*x-y*, 1 by 1 μm; *z*-range, 3 nN) (B, E, H, K, and N) and corresponding adhesion histograms ($n = 1{,}024$) (C, F, I, L, and O) recorded with hydrophobic tips on the surfaces of Δ*pksP* (A to C), Δ*ayg1* (D to F), Δ*arp2* (G to I), Δ*arp1* (J to L), and WT (M to O) conidia.

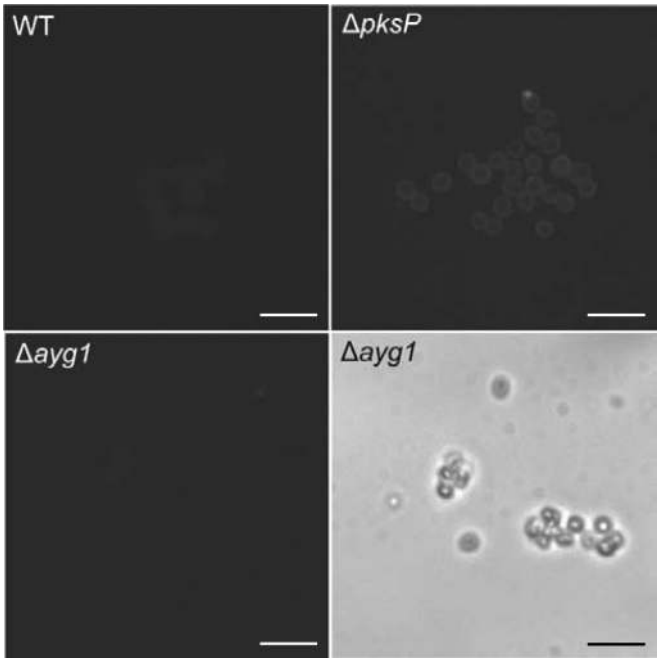

FIG 8 ConA-FITC labeling of Δ*pksP*, Δ*ayg1*, and WT strain resting conidia. Note the increase in ConA labeling on the Δ*pksP* mutant conidial surface compared to WT and Δ*ayg1* conidia. Scale bar, 10 μm.

secreted proteins, which otherwise secreted normally during conidial germination, and exposed the GlcN polymers on the conidial surfaces. Proteins and GlcN polymers were responsible for the DC activation after incubation of cells with Δ*pksP*, Δ*ayg1*, and Δ*arp2* conidia. The Δ*abr1* and Δ*abr2* conidia were immunologically inert like their WT counterparts, whereas Δ*arp1* conidia presented an intermediate phenotype.

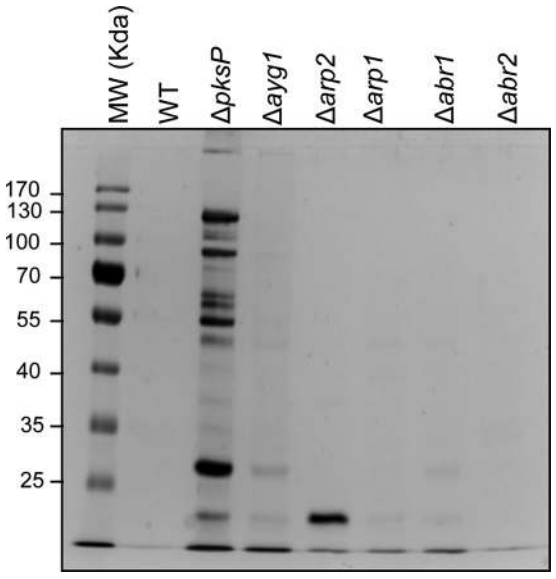

FIG 9 NaCl-extracted proteins from the surfaces of mutant and WT resting conidia. SDS-PAGE (10% gel) of proteins extracted after 2 h of incubation of resting conidia in 0.5 M NaCl was performed.

TABLE 1 Identification of proteins extracted from the Δ*pksP* mutant conidial surface[a]

Locus tag[b]	Protein sequence identification no.	Name
AFUA_6G12070	gi|70992475	FAD binding domain protein
AFUA_5G09580	gi|83305637	Hydrophobin RodAp
AFUA_3G02270	gi|70986104	Mycelial catalase Cat1p
AFUA_8G00630	gi|70983229	Conserved hypothetical protein
AFUA_1G05770	gi|70990956	Exo-β-1,3-glucosidase ExoG2p
AFUA_4G09280	gi|70994100	Conserved hypothetical protein
AFUA_1G03600	gi|70990522	Exo-β-1,3-glucanase Exg1p
AFUA_3G15090	gi|146323525	Adenosine deaminase family protein
AFUA_2G11440	gi|71001590	Proteasome component Pup2p
AFUA_6G06350	gi|70991357	Proteasome subunit alpha type 3
AFUA_6G04790	gi|70984160	Proteasome component Pre5p
AFUA_7G04650	gi|70987129	Proteasome component Pre3p
AFUA_3G11300	gi|70999540	Proteasome component Prs2p
AFUA_6G06450	gi|70991377	Proteasome component Pre4p
AFUB_042910	gi|159128006	Cytoskeleton assembly control protein Sla2p, putative
AFUA_7G06140	gi|70986816	Putative secreted 1,4-β-D-glucan glucanhydrolase
AFUA_1G12610	gi|70995752	Hsp70 chaperone Hsp88p
AFUA_8G05020	gi|70983560	β-*N*-Acetylhexosaminidase NagAp
AFUA_1G14560	gi|70996140	Mannosidase MsdSp
AFUA_5G12780	gi|70997246	Kelch repeat protein
AFUA_2G10660	gi|71001436	Mannitol-1-phosphate dehydrogenase
AFUA_6G06440	gi|70991375	Proteasome component Prs3p
AFUA_5G02330	gi|70985206	Major allergen and cytotoxin AspF1
AFUA_1G13670	gi|70995964	Conserved hypothetical protein
AFUA_3G13465	gi|146323476	Conserved hypothetical protein
AFUA_2G11900	gi|71001682	Pyruvate dehydrogenase kinase
AFUA_4G03490	gi|70982015	Tripeptidyl-peptidase (TppAp)
AFUA_1G04130	gi|70985206	FG-GAP repeat protein
AFUA_3G00590	gi|70985747	Asp-hemolysin
AFUB_018320	gi|159128674	β-Fructofuranosidase, putative
AFUA_1G12170	gi|70995660	Translation elongation factor EF-Tu
AFUA_5G00700	gi|70985526	Hypothetical protein AFUA_5G00700
AFUA_8G01980	gi|70982961	Conserved hypothetical protein
AFUA_1G13670	gi|70995964	Conserved hypothetical protein
AFUA_2G06150	gi|70989789	Protein disulfide isomerase Pdi1p
AFUA_6G04570	gi|70984206	Translation elongation factor eEF-1 subunit gamma
AFLA_093140	gi|238499799	Histone H3 methyltransferase, putative
AFUA_3G07810	gi|71000275	Succinate dehydrogenase subunit Sdh1p
AFUA_8G01410	gi|70983075	Class V chitinase ChiB1p
AFUA_3G11690	gi|70999466	Fructose-bisphosphate aldolase, class II
AFUB_007340	gi|159130919	Pyruvate dehydrogenase E1 component α-subunit, putative

[a] Identification was accomplished using MS/MS and MS with a mascot score above a threshold of 54.
[b] *A. fumigatus* locus tag (www.aspergillusgenome.org).

DISCUSSION

In fungal biology, melanin pigments are attributed with a variety of beneficial functions, including protection against exogenous stress, UV irradiation, and host defense mechanisms, including reactive oxygen species, lytic enzymes, and antimicrobial peptides (47), and hence considered to be one of the fungal virulence factors (48). Melanin, being extracellular, also contributes to the fungal spore structure (5). In *A. fumigatus*, melanin biosynthesis is reported to require a cluster of six genes (6, 13, 14). In the present study, we show for the first time the effect of the deletion of individual genes from the melanin biosynthetic gene cluster on the respective conidial surface morphology and the consequent immune responses to the mutant conidia.

The mutant conidia with a deletion in one of the first three genes of the melanin pathway (Δ*pksP*, Δ*ayg1*, and Δ*arp2*) stimu-

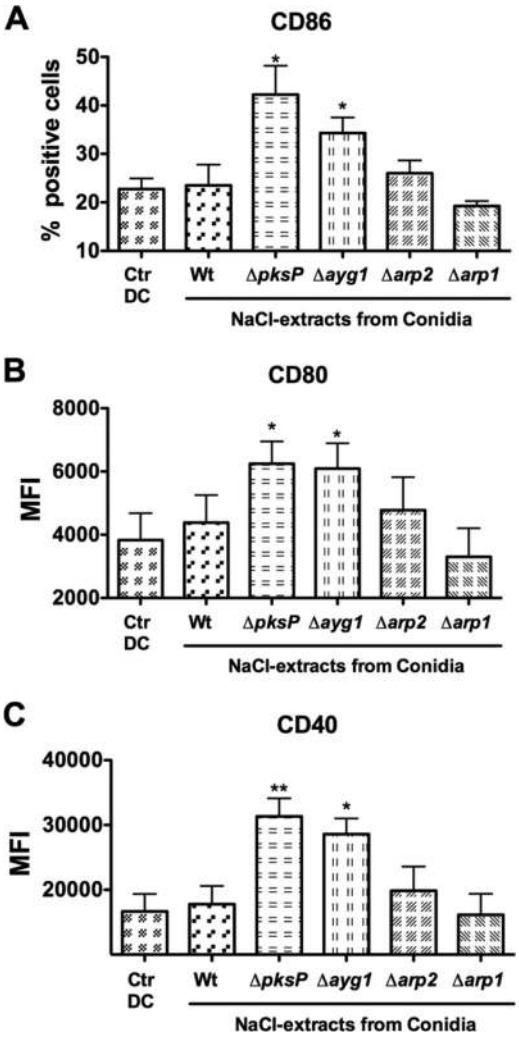

FIG 10 Effect of NaCl extracts from the surfaces of mutant and WT resting conidia on the maturation of DCs. Immature DCs were cultured in the presence of the cytokines GM-CSF and IL-4 (Ctr DC) or cytokines and NaCl-extracts from the surfaces of WT resting conidia or mutant conidia (Δ*pksP*, Δ*ayg1*, Δ*arp2*, and Δ*arp1*) for 48 h. The percent expression of CD86 (A) and the mean fluorescence intensities (MFI) of CD80 (B) and CD40 (C) were analyzed by flow cytometry. The data (means ± the SEM) are from four donors. The level of statistical significance is indicated (*, $P < 0.05$, **, $P < 0.01$).

lated the maturation and elicited the production of IL-6, IL-1β, TNF-α, and IL-10 cytokines by DCs, whereas Δ*abr1*, Δ*abr2*, and WT conidia were not immunogenic. The Δ*arp1* mutant presented an intermediate phenotype since it induced partial activation of the DCs. Melanins as such were immunologically inert since the melanin ghost extracted from the WT conidia failed to activate DCs. These results suggested that the surfaces of Δ*pksP*, Δ*ayg1*, and Δ*arp2* resting conidia are covered with specific common compounds that are rare in Δ*arp1* conidia and are responsible for the maturation of DCs.

The major obvious phenotypes of Δ*pksP*, Δ*ayg1*, and Δ*arp2* resting conidia were the absence or very few patches of rodlets at the surface. Although the rodlets that immune-silence the resting conidia were present in the above mutant conidia, the masking of rodlets by an amorphous and hydrophilic layer enabled resting conidia to be immunogenic (24, 49). A few patches of amorphous and hydrophilic layers could also be observed on the Δ*arp1* conidial surface. When downstream genes of the DHN-melanin pathway were deleted, the appearance of the rodlets and the hydrophobicity of the conidia increased. Previous studies demonstrated that deletion of *PKSP* and *ARP2* correlated with a decreased ability to bind laminin on the conidial surface (10). This result is explained by the low hydrophobicity of the conidia, which reduced the electronegative charge required for laminin binding.

The amorphous and hydrophilic layer is composed of GlcN-containing components and deposited ConA-positive proteins mostly in Δ*pksP* conidia. These proteins were analyzed in the Δ*pksP* mutant, and their identification showed that they are usually secreted during vegetative growth. Most hydrolases (such as β-1,3-glucosidases, β-*N*-acetylhexosaminidase, and mannosidase), catalase, Aspf1, Asp-hemolysin, and chitinase found in the amorphous surface layer of the resting Δ*pksP* conidia were usually identified during mycelial growth in a protein-based medium (43–46). Their presence on the surfaces of resting conidia of Δ*pksP* and Δ*ayg1* mutants is explained by modifications of the ionic strength of the hydrophobin layer resulting from the absence of melanin or at least the YWA1, a melanin biosynthetic intermediate that is synthesized by the combined activities of PksPp and Ayg1p. The easy removal of these hydrophilic glycoproteins by 0.5 M NaCl suggested that they adhered to the conidial cell wall through electrostatic binding. These surface proteins in the conidial amorphous layers were responsible for the DC maturation and cytokine production. Interestingly, cell wall structural modifications resulting from the absence of α-(1,3)-glucan, as in *A. fumigatus* Δ*ags1* Δ*ags2* Δ*ags3* (Δ*ags*) mutant, also gave the similar conidial phenotype, a hydrophilic protein layer on the surface of the conidia that stimulated host defense reactions (24). However, the composition of proteins in this amorphous layer in triple Δ*ags* and Δ*pksP* deletion mutants was not the same, suggesting defined cell wall permeability defects due to the deletion of different cell wall component biosynthetic genes. When the melanin synthesis pathway was blocked farther downstream by gene deletion, fewer proteins were able to cross the conidial cell wall. Of note, DC cytokine production was less for Δ*pksP* mutant than for Δ*ayg1* and Δ*arp2* mutant conidia (Fig. 3). This result suggests that glycoproteins were less stimulatory than GlcN residues present on the surfaces of the Δ*pksP*, Δ*ayg1*, and Δ*arp2* mutant conidia and that these GlcN residues are less exposed on Δ*pksP* mutant surfaces due to the larger amount of glycoproteins in this mutant.

The presence of GlcN residues on the surfaces of the Δ*pksP*, Δ*ayg1*, and Δ*arp2* mutant conidia could be explained by the unmasking of cell wall chitin due to the absence of melanin. The hexosamines present in the conidial cell wall were composed of long chains of fibrillar water insoluble chitin, amorphous and soluble chitin oligosaccharides (containing 10 to 15 *N*-acetylglucosamines), and deacetylated chitin (chitosan) (A. Beauvais et al., unpublished results). Previous studies on different-sized chitin polymers have shown that >70-μm chitin polymers were immunologically inert with murine macrophages, whereas both intermediate-sized (40- to 70-μm) and small (<40-μm) chitin polymers stimulated TNF elaboration by macrophages (50), and only <40-μm chitin polymers induced IL-10 production. Small particles of chitosan were even better macrophage immune stimulators. Chitosan of <20 μm elicited the most IL-1β from bone marrow-derived macrophages (50). Although several chitin-binding

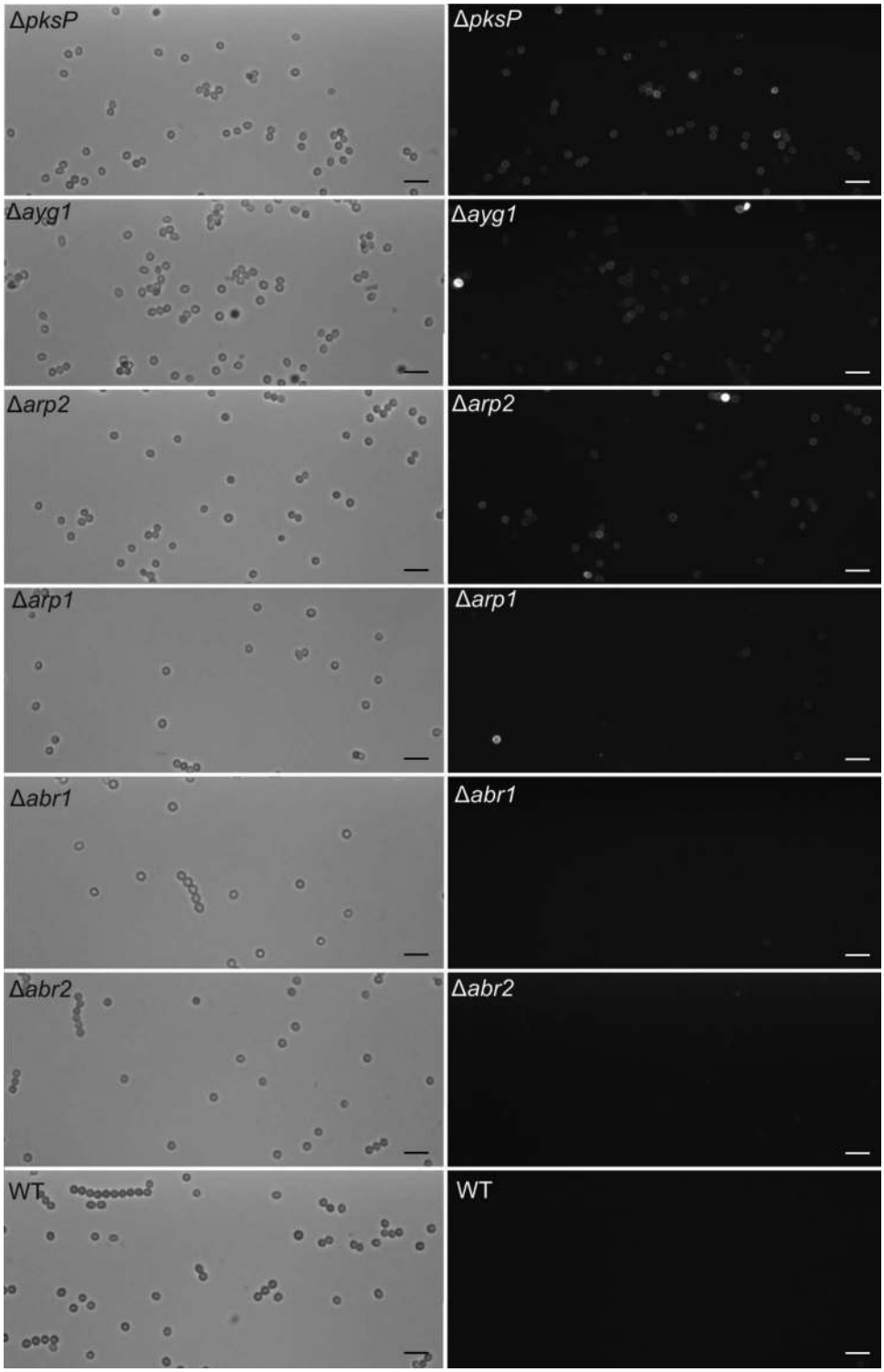

FIG 11 WGA-FITC labeling of mutant and WT resting conidia. Note the decreasing numbers of ConA-positive conidia from the first mutants of the melanin pathway to the last one. Scale bar, 10 μm.

proteins have been identified in mammalian cells, no chitin receptor had thus far been identified thus far. A recent study on the recognition of innate immune cells by *Candida albicans* chitin revealed that although there was no direct dectin-1 and chitin binding, chitin was capable of blocking dectin-1-mediated immune responses (51). Similarly, these small and/or deacetylated chitins were likely unmasked on the surfaces of the first three melanin mutants and were responsible for the DC maturation. Such an unmasking phenomenon was reported in chitin synthase Δ*csmA* and Δ*csmB* mutants, wherein the deletion of two of the

chitin synthase genes (*CSMA* and *CSMB*) in *A. fumigatus* resulted in the increased exposure of WGA-positive components on the conidial surfaces (42). The Δ*csmA* conidial surface was also amorphous and ConA positive; however, ConA-positive materials were not glycoproteins but rather due to the exposure of mannan-containing polymers. This further confirms the differential permeability defects due to the deletion of specific cell wall component biosynthetic genes.

Chai et al. (9) also demonstrated that melanin purified from WT conidia was also poorly immunogenic for the stimulation of cytokines by peripheral blood mononuclear cells. On the other hand, as seen in our study, Δ*pksP* conidia elicited significantly higher cytokine production, including IL-10, IL-6, and TNF-α. These researchers found that the blockage of dectin-1 with laminarin reduced cytokine production in response to Δ*pksP* conidia, which could be correlated with WGA-FITC positivity of Δ*pksP*, Δ*ayg1*, and Δ*arp2* mutant conidia and the observations that chitin can influence dectin-1-mediated immune responses (51). Jahn et al. (52) observed that the extent of macrophage phagocytosis and intracellular killing was significantly greater with Δ*pksP* conidia than with WT conidia. Thywissen et al. (18) showed that inside the phagolysosome, WT conidial DHN-melanin was responsible for the inhibition of the phagolysosomal acidification of mouse and human macrophages and neutrophils. The Δ*pksP* conidia, in contrast, were located in an acidic environment in the phagolysosome, which coincides with more effective killing of these conidia. The percentages of Δ*ayg1*, Δ*arp2*, and Δ*abr2* conidia were lower in acidified phagolysosomes than those of Δ*pksP* conidia but higher than those of WT conidia. These results show that melanin intermediates formed by the downstream biosynthetic pathway increase conidial protection. However, the final product, the DHN-melanin, was important for the maximal protection since it facilitates the formation of a complete surface rodlet layer that hides conidia from their immediate recognition by the immune system.

Conclusion. The absence of at least the scytalone intermediate of DHN-melanin is responsible for structural and chemical modifications of the cell surface, which will have an obvious impact on the immune response of the host toward the corresponding mutant. Our results also show that melanin is essential to acquire the right surface properties with precise charge and hydrophobicity that are necessary to have immunologically inert conidia due to an exposed rodlet layer.

ACKNOWLEDGMENTS

We thank Maria Pötsch for excellent technical support.

This study was partly supported by Aviesan grant BA-P1-09 Aspergillus. Research in the Unité des Aspergillus, Institut Pasteur, and the Institut National de la Santé et de la Recherche Médicale Unité 1138 was supported by European Community's Seventh Framework Programme (FP7/2007-2013) under grant agreement 260338 ALLFUN and ANR-10-BLAN-1309 HYDROPHOBIN. Work at the Université Catholique de Louvain was supported by the National Fund for Scientific Research, the Université Catholique de Louvain (Fonds Spéciaux de Recherche), the Federal Office for Scientific, Technical, and Cultural Affairs (Interuniversity Poles of Attraction Programme), and the Research Department of the Communauté Française de Belgique (Concerted Research Action).

The funders had no role in study design, data collection and analysis, decision to publish, or preparation of the manuscript.

REFERENCES

1. **Rosa LH, de Almeida Vieira ML, Santiago IF, Rosa CA.** 2010. Endophytic fungi community associated with the dicotyledonous plant *Colobanthus quitensis* (Kunth) Bartl. (*Caryophyllaceae*) in Antarctica. FEMS Microbiol. Ecol. **73:**178–189. http://dx.doi.org/10.1111/j.1574-6941.2010.00872.x.
2. **Zalar P, Novak M, de Hoog GS, Gunde-Cimerman N.** 2011. Dishwashers: a man-made ecological niche accommodating human opportunistic fungal pathogens. Fungal Biol. **115:**997–1007. http://dx.doi.org/10.1016/j.funbio.2011.04.007.
3. **Ngamskulrungroj P, Price J, Sorrell T, Perfect JR, Meyer W.** 2011. *Cryptococcus gattii* virulence composite: candidate genes revealed by microarray analysis of high and less virulent Vancouver island outbreak strains. PLoS One **6:**e16076. http://dx.doi.org/10.1371/journal.pone.0016076.
4. **Volling K, Thywissen A, Brakhage AA, Saluz HP.** 2011. Phagocytosis of melanized *Aspergillus* conidia by macrophages exerts cytoprotective effects by sustained PI3K/Akt signaling. Cell. Microbiol. **13:**1130–1148. http://dx.doi.org/10.1111/j.1462-5822.2011.01605.x.
5. **Jahn B, Koch A, Schmidt A, Wanner G, Gehringer H, Bhakdi S, Brakhage AA.** 1997. Isolation and characterization of a pigmentless-conidium mutant of *Aspergillus fumigatus* with altered conidial surface and reduced virulence. Infect. Immun. **65:**5110–5117.
6. **Tsai HF, Wheeler MH, Chang YC, Kwon-Chung KJ.** 1999. A developmentally regulated gene cluster involved in conidial pigment biosynthesis in *Aspergillus fumigatus*. J. Bacteriol. **181:**6469–6477.
7. **Schmaler-Ripcke J, Sugareva V, Gebhardt P, Winkler R, Kniemeyer O, Heinekamp T, Brakhage AA.** 2009. Production of pyomelanin, a second type of melanin, via the tyrosine degradation pathway in *Aspergillus fumigatus*. Appl. Environ. Microbiol. **75:**493–503. http://dx.doi.org/10.1128/AEM.02077-08.
8. **Eisenman HC, Casadevall A.** 2012. Synthesis and assembly of fungal melanin. Appl. Microbiol. Biotechnol. **93:**931–940. http://dx.doi.org/10.1007/s00253-011-3777-2.
9. **Chai LY, Netea MG, Sugui J, Vonk AG, van de Sande WW, Warris A, Kwon-Chung KJ, Kullberg BJ.** 2010. *Aspergillus fumigatus* conidial melanin modulates host cytokine response. Immunobiology **215:**915–920. http://dx.doi.org/10.1016/j.imbio.2009.10.002.
10. **Pihet M, Vandeputte P, Tronchin G, Renier G, Saulnier P, Georgeault S, Mallet R, Chabasse D, Symoens F, Bouchara JP.** 2009. Melanin is an essential component for the integrity of the cell wall of *Aspergillus fumigatus* conidia. BMC Microbiol. **9:**177. http://dx.doi.org/10.1186/1471-2180-9-177.
11. **Keller S, Macheleidt J, Scherlach K, Schmaler-Ripcke J, Jacobsen ID, Heinekamp T, Brakhage AA.** 2011. Pyomelanin formation in *Aspergillus fumigatus* requires HmgX and the transcriptional activator HmgR but is dispensable for virulence. PLoS One **6:**e26604. http://dx.doi.org/10.1371/journal.pone.0026604.
12. **Sugareva V, Hartl A, Brock M, Hubner K, Rohde M, Heinekamp T, Brakhage AA.** 2006. Characterisation of the laccase-encoding gene *abr2* of the dihydroxynaphthalene-like melanin gene cluster of *Aspergillus fumigatus*. Arch. Microbiol. **186:**345–355. http://dx.doi.org/10.1007/s00203-006-0144-2.
13. **Tsai HF, Fujii I, Watanabe A, Wheeler MH, Chang YC, Yasuoka Y, Ebizuka Y, Kwon-Chung KJ.** 2001. Pentaketide melanin biosynthesis in *Aspergillus fumigatus* requires chain-length shortening of a heptaketide precursor. J. Biol. Chem. **276:**29292–29298. http://dx.doi.org/10.1074/jbc.M101998200.
14. **Tsai HF, Washburn RG, Chang YC, Kwon-Chung KJ.** 1997. *Aspergillus fumigatus arp1* modulates conidial pigmentation and complement deposition. Mol. Microbiol. **26:**175–183. http://dx.doi.org/10.1046/j.1365-2958.1997.5681921.x.
15. **Fujii I, Yasuoka Y, Tsai HF, Chang YC, Kwon-Chung KJ, Ebizuka Y.** 2004. Hydrolytic polyketide shortening by Ayg1p, a novel enzyme involved in fungal melanin biosynthesis. J. Biol. Chem. **279:**44613–44620. http://dx.doi.org/10.1074/jbc.M406758200.
16. **Langfelder K, Jahn B, Gehringer H, Schmidt A, Wanner G, Brakhage AA.** 1998. Identification of a polyketide synthase gene (*pksP*) of *Aspergillus fumigatus* involved in conidial pigment biosynthesis and virulence. Med. Microbiol. Immunol. **187:**79–89. http://dx.doi.org/10.1007/s004300050077.
17. **Slesiona S, Gressler M, Mihlan M, Zaehle C, Schaller M, Barz D, Hube B, Jacobsen ID, Brock M.** 2012. Persistence versus escape: *Aspergillus terreus* and *Aspergillus fumigatus* employ different strategies during interactions with macrophages. PLoS One **7:**e31223. http://dx.doi.org/10.1371/journal.pone.0031223.
18. **Thywissen A, Heinekamp T, Dahse HM, Schmaler-Ripcke J, Nietzsche**

S, Zipfel PF, Brakhage AA. 2011. Conidial dihydroxynaphthalene melanin of the human pathogenic fungus *Aspergillus fumigatus* interferes with the host endocytosis pathway. Front. Microbiol. **2:**96. http://dx.doi.org/10.3389/fmicb.2011.00096.

19. **Luther K, Torosantucci A, Brakhage AA, Heesemann J, Ebel F.** 2007. Phagocytosis of *Aspergillus fumigatus* conidia by murine macrophages involves recognition by the dectin-1 β-glucan receptor and Toll-like receptor 2. Cell. Microbiol. **9:**368–381. http://dx.doi.org/10.1111/j.1462-5822.2006.00796.x.
20. **Rosas AL, Nosanchuk JD, Gomez BL, Edens WA, Henson JM, Casadevall A.** 2000. Isolation and serological analyses of fungal melanins. J. Immunol. Methods **244:**69–80. http://dx.doi.org/10.1016/S0022-1759(00)00255-6.
21. **Youngchim S, Morris-Jones R, Hay RJ, Hamilton AJ.** 2004. Production of melanin by *Aspergillus fumigatus*. J. Med. Microbiol. **53:**175–181. http://dx.doi.org/10.1099/jmm.0.05421-0.
22. **Beauvais A, Maubon D, Park S, Morelle W, Tanguy M, Huerre M, Perlin DS, Latgé JP.** 2005. Two α(1,3)-glucan synthases with different functions in *Aspergillus fumigatus*. Appl. Environ. Microbiol. **71:**1531–1538. http://dx.doi.org/10.1128/AEM.71.3.1531-1538.2005.
23. **Aimanianda V, Clavaud C, Simenel C, Fontaine T, Delepierre M, Latge JP.** 2009. Cell wall β-(1,6)-glucan of *Saccharomyces cerevisiae*: structural characterization and in situ synthesis. J. Biol. Chem. **284:**13401–13412. http://dx.doi.org/10.1074/jbc.M807667200.
24. **Beauvais A, Bozza S, Kniemeyer O, Formosa C, Balloy V, Henry C, Roberson RW, Dague E, Chignard M, Brakhage AA, Romani L, Latgé JP.** 2013. Deletion of the α-(1,3)-glucan synthase genes induces a restructuring of the conidial cell wall responsible for the avirulence of *Aspergillus fumigatus*. PLoS Pathog. **9:**e1003716. http://dx.doi.org/10.1371/journal.ppat.1003716.
25. **Kniemeyer O, Lessing F, Scheibner O, Hertweck C, Brakhage AA.** 2006. Optimisation of a 2-D gel electrophoresis protocol for the human-pathogenic fungus *Aspergillus fumigatus*. Curr. Genet. **49:**178–189. http://dx.doi.org/10.1007/s00294-005-0047-9.
26. **Muller S, Baldin C, Groth M, Guthke R, Kniemeyer O, Brakhage AA, Valiante V.** 2012. Comparison of transcriptome technologies in the pathogenic fungus *Aspergillus fumigatus* reveals novel insights into the genome and MpkA-dependent gene expression. BMC Genomics **13:**519. http://dx.doi.org/10.1186/1471-2164-13-519.
27. **Lamarre C, Beau R, Balloy V, Fontaine T, Wong Sak Hoi J, Guadagnini S, Berkova N, Chignard M, Beauvais A, Latgé JP.** 2009. Galactofuranose attenuates cellular adhesion of *Aspergillus fumigatus*. Cell. Microbiol. **11:**1612–1623. http://dx.doi.org/10.1111/j.1462-5822.2009.01352.x.
28. **Steele C, Rapaka RR, Metz A, Pop SM, Williams DL, Gordon S, Kolls JK, Brown GD.** 2005. The β-glucan receptor dectin-1 recognizes specific morphologies of *Aspergillus fumigatus*. PLoS Pathog. **1:**e42. http://dx.doi.org/10.1371/journal.ppat.0010042.
29. **Bansal K, Sinha AY, Ghorpade DS, Togarsimalemath SK, Patil SA, Kaveri SV, Balaji KN, Bayry J.** 2010. Src homology 3-interacting domain of Rv1917c of *Mycobacterium tuberculosis* induces selective maturation of human dendritic cells by regulating PI3K-MAPK-NF-κB signaling and drives Th2 immune responses. J. Biol. Chem. **285:**36511–36522. http://dx.doi.org/10.1074/jbc.M110.158055.
30. **Aimanianda V, Bayry J, Bozza S, Kniemeyer O, Perruccio K, Elluru SR, Clavaud C, Paris S, Brakhage AA, Kaveri SV, Romani L, Latgé JP.** 2009. Surface hydrophobin prevents immune recognition of airborne fungal spores. Nature **460:**1117–11121. http://dx.doi.org/10.1038/nature08264.
31. **Bansal K, Elluru SR, Narayana Y, Chaturvedi R, Patil SA, Kaveri SV, Bayry J, Balaji KN.** 2010. PE_PGRS antigens of *Mycobacterium tuberculosis* induce maturation and activation of human dendritic cells. J. Immunol. **184:**3495–3504. http://dx.doi.org/10.4049/jimmunol.0903299.
32. **Alsteens D, Dague E, Rouxhet PG, Baulard AR, Dufrene YF.** 2007. Direct measurement of hydrophobic forces on cell surfaces using AFM. Langmuir **23:**11977–11979. http://dx.doi.org/10.1021/la702765c.
33. **Dufrene YF.** 2008. Atomic force microscopy and chemical force microscopy of microbial cells. Nat. Protoc. **3:**1132–1138. http://dx.doi.org/10.1038/nprot.2008.101.
34. **Banchereau J, Steinman RM.** 1998. Dendritic cells and the control of immunity. Nature **392:**245–252. http://dx.doi.org/10.1038/32588.
35. **Cella M, Scheidegger D, Palmer-Lehmann K, lane P, Lanzavecchia A, Alber G.** 1996. Ligation of CD40 on dendritic cells triggers production of high levels of interleukin-12 and enhances T cell stimulatory capacity: T-T help via APC activation. J. Exp. Med. **184:**747–752. http://dx.doi.org/10.1084/jem.184.2.747.
36. **Dufrene YF, Boonaert CJ, Gerin PA, Asther M, Rouxhet PG.** 1999. Direct probing of the surface ultrastructure and molecular interactions of dormant and germinating spores of *Phanerochaete chrysosporium*. J. Bacteriol. **181:**5350–5354.
37. **Dufrene YF.** 2004. Using nanotechniques to explore microbial surfaces. Nat. Rev. Microbiol. **2:**451–460. http://dx.doi.org/10.1038/nrmicro905.
38. **Andre G, Kulakauskas S, Chapot-Chartier MP, Navet B, Deghorain M, Bernard E, Hols P, Dufrêne YF.** 2010. Imaging the nanoscale organization of peptidoglycan in living *Lactococcus lactis* cells. Nat. Commun. **1:**27. http://dx.doi.org/10.1038/ncomms1027.
39. **Alsteens D, Trabelsi H, Soumillion P, Dufrene YF.** 2013. Multiparametric atomic force microscopy imaging of single bacteriophages extruding from living bacteria. Nat. Commun. **4:**2926. http://dx.doi.org/10.1038/ncomms3926.
40. **Beaussart A, Alsteens D, El-Kirat-Chatel S, Lipke PN, Kucharikova S, Van Dijck P, Dufrêne YF.** 2012. Single-molecule imaging and functional analysis of Als adhesins and mannans during *Candida albicans* morphogenesis. ACS Nano. **6:**10950–10964. http://dx.doi.org/10.1021/nn304505s.
41. **Dague E, Alsteens D, Latge JP, Verbelen C, Raze D, Baulard AR, Dufrêne YF.** 2007. Chemical force microscopy of single live cells. Nano Lett. **7:**3026–3030. http://dx.doi.org/10.1021/nl071476k.
42. **Alsteens D, Aimanianda V, Hegde P, Pire S, Beau R, Bayry J, Latgé JP, Dufrêne YF.** 2013. Unraveling the nanoscale surface properties of chitin synthase mutants of *Aspergillus fumigatus* and their biological implications. Biophys. J. **105:**320–327. http://dx.doi.org/10.1016/j.bpj.2013.05.040.
43. **Alcazar-Fuoli L, Clavaud C, Lamarre C, Aimanianda V, Seidl-Seiboth V, Mellado E, Latgé JP.** 2011. Functional analysis of the fungal/plant class chitinase family in *Aspergillus fumigatus*. Fungal Genet. Biol. **48:**418–429. http://dx.doi.org/10.1016/j.fgb.2010.12.007.
44. **Singh B, Oellerich M, Kumar R, Kumar M, Bhadoria DP, Reichard U, Gupta VK, Sharma GL, Asif AR.** 2010. Immunoreactive molecules identified from the secreted proteome of *Aspergillus fumigatus*. J. Proteome Res. **9:**5517–5529. http://dx.doi.org/10.1021/pr100604x.
45. **Sriranganadane D, Waridel P, Salamin K, Reichard U, Grouzmann E, Neuhaus M, Quadroni JM, Monod M.** 2010. Aspergillus protein degradation pathways with different secreted protease sets at neutral and acidic pH. J. Proteome Res. **9:**3511–3519. http://dx.doi.org/10.1021/pr901202z.
46. **Wartenberg D, Lapp K, Jacobsen ID, Dahse HM, Kniemeyer O, Heinekamp T, Brakhage AA.** 2011. Secretome analysis of *Aspergillus fumigatus* reveals Asp-hemolysin as a major secreted protein. Int. J. Med. Microbiol. **301:**602–611. http://dx.doi.org/10.1016/j.ijmm.2011.04.016.
47. **Heinekamp T, Thywissen A, Macheleidt J, Keller S, Valiante V, Brakhage AA.** 2012. *Aspergillus fumigatus* melanins: interference with the host endocytosis pathway and impact on virulence. Front. Microbiol. **3:**440. http://dx.doi.org/10.3389/fmicb.2012.00440.
48. **Buskirk AD, Templeton SP, Nayak AP, Hettick JM, Law BF, Green BJ, Beezhold DH.** 2014. Pulmonary immune responses to *Aspergillus fumigatus* in an immunocompetent mouse model of repeated exposures. J. Immunotoxicol. **11:**180–189. http://dx.doi.org/10.3109/1547691X.2013.819054.
49. **Jimenez-Ortigosa C, Aimanianda V, Muszkieta L, Mouyna I, Alsteens D, Pire S, Beau R, Krappmann S, Beauvais A, Dufrêne YF, Roncero C, Latgé JP.** 2012. Chitin synthases with a myosin motor-like domain control the resistance of *Aspergillus fumigatus* to echinocandins. Antimicrob. Agents Chemother. **56:**6121–6131. http://dx.doi.org/10.1128/AAC.00752-12.
50. **Bueter CL, Lee CK, Rathinam VA, Healy GJ, Taron CH, Specht CA, Levitz SM.** 2011. Chitosan but not chitin activates the inflammasome by a mechanism dependent upon phagocytosis. J. Biol. Chem. **286:**35447–35455. http://dx.doi.org/10.1074/jbc.M111.274936.
51. **Mora-Montes HM, Netea MG, Ferwerda G, Lenardon MD, Brown GD, Mistry AR, Kullberg BJ, O'Callaghan CA, Sheth CC, Odds FC, Brown AJ, Munro CA, Gow NA.** 2011. Recognition and blocking of innate immunity cells by *Candida albicans* chitin. Infect. Immun. **79:**1961–1970. http://dx.doi.org/10.1128/IAI.01282-10.
52. **Jahn B, Langfelder K, Schneider U, Schindel C, Brakhage AA.** 2002. PKSP-dependent reduction of phagolysosome fusion and intracellular kill of *Aspergillus fumigatus* conidia by human monocyte-derived macrophages. Cell. Microbiol. **4:**793–803. http://dx.doi.org/10.1046/j.1462-5822.2002.00228.x.